Polymer Bulletin 56, 455–466 (2006)
DOI 10.1007/s00289-005-0499-6

Polymer Bulletin

Phase Behavior and its Viscoelastic Responses of Poly(methyl methacrylate) and Poly(styrene-co-maleic anhydride) Blend Systems

Runming Li[1, 2], Wei Yu[1], Chixing Zhou[1] (✉)

[1] College of Chemistry and Chemical Engineering, Shanghai Jiao Tong University, Shanghai 200240, China
[2] College of Chemistry and Chemical Engineering, Henan University, Kaifeng 475001, China

e-mail: cxzhou@sjtu.edu.cn

Received: 10 November 2005 / Revised version: 15 December 2005 / Accepted: 20 December 2005
Published online: 9 January 2006 –

Summary

The phase behavior and viscoelastic properties of the poly(methyl methacrylate) (PMMA) and poly(styrene-co-maleic anhydride) (SMA) blend systems have been investigated. In homogeneous region, the blends of different compositions behave as a classical polymer melt. On the other hand, in phase-separated region, the blends of symmetric and off-symmetric compositions show different characteristic thermorheological responses corresponding to the different morphologies, which has been confirmed by TEM analysis and qualitatively corroborated by utilizing Palierne's emulsion model. Except for the well-known characteristic deviations of the storage modulus at low frequencies, the curves that describe the relationships between other rheological functions such as master curves obtained through time-temperature superposition (tTS) principle, van Gurp-Palmen Plots, Han Plots, and Cole-Cole Plots, also show significantly different shapes corresponding to symmetric and off-symmetric composition. Based on these findings we propose that such characteristic fingerprints can be used not only for marking phase separation but also for inferring the resulting morphology. It is also shown that van Gurp-Palmen Plots and Cole-Cole Plots are more sensitive than other rheological functions. In addition, on comparing the validity of tTS principle in different blend systems, we argue that the morphology is responsible for whether tTS principle holds or not for polymer blend.

Introduction

Mixing different polymers can lead to a wide range of phase behaviors that directly influence the associated physical properties and ultimate applications [1]. For a partially miscible polymer pair, phase behavior is determined by two key factors: composition and temperature. For a mixture of certain composition, thermally induce phase separation can proceed by two different mechanisms: nucleation and growth (NG), or spinodal decomposition (SD), which results in different types of morphologies: droplet-matrix or co-continuous morphology, respectively. The associated viscoelastic properties show complex behaviors in general [2-23]. In return,

these characteristic rheological responses might give helpful information on the internal structure of such materials. In fact, rheology is so sensitive that it can be use to determine the miscibility [2, 5, 7, 11, 14-16], to trace the kinetics of phase separation [8, 9], and to evaluate morphology [24-26]. It was shown that for the blend with a co-continuous structure, the storage modulus shows a power law behavior in the low frequency ranges [8, 13, 23], and for the blend with a droplet-matrix one, the presence of a dispersed droplet phase leads to an increase in elasticity at low frequencies due to extra stresses, causing a shoulder in the storage modulus versus frequency curve [8, 23]. These results are instructive for us to understand the relationship between the rheological properties and structure. However, up to now, many investigations have been only focusing on the viscoelastic dynamic moduli, and there is yet a lack of complete correlation between structure and its rheological response.

In the present paper, we report on the linear viscoelastic behavior of partially miscible blend of poly(methyl methacrylate) (PMMA) and poly(styrene-co-maleic anhydride) (SMA) blends of symmetric and off-symmetric composition in homogenous and phase-separated regions as measured in small amplitude oscillatory shear (SAOS) mode. Our aim is to manifest rheological responses of the blend with different internal structure. This is one step in the endeavor to establish a satisfactory criterion for the characterization of phase structure by rheology.

Experimental

Materials

Poly(methyl methacrylate) (PMMA G66) was supplied from BASF. Poly(styrene-*co*-maleic anhydride) (SMA), containing 12 wt % of maleic anhydride, was donated by SINOPEC Shanghai Research Institute of Petrochemical Technology. The weight-average molecular weight and polydispersity were determined by the gel permeation chromatography (GPC) (Perkin Elmer Series 200). Thermal analysis was carried out using differential scanning calorimetry (DSC) (Perkin Elmer PYRIS-1). The material parameters are listed in Table 1.

Table 1 Characteristics of the polymers used in this study

Polymer	M_w	M_w/M_n	T_g (^oC)
PMMA	72,400	2.0	95.0
SMA	191,300	2.5	126.5

Preparation of Blends

Prior to melt mixing, all polymers were dried in vacuum at 80^{o}C for at least 24hours. Blends of PMMA/SMA were prepared by melt blending on the Haake Rheocord 99 with Rheomix 60 mixer at 180^{o}C and 40rpm. The mixing continued until a constant torque was reached, which took about 15-20min. The samples for rheological testing were prepared by compression molding at 180^{o}C for about an hour in the form of 25mm diameter disks with 1.5mm in thickness. To avoid water absorption, the blends obtained were stored in a vacuum oven at 80^{o}C for at least two days before usage. All samples are optical transparent, and this indicates that they are miscible.

Turbidity

Turbidity measurements were performed on a simple self-made heating block. In addition, transmitted intensity measurements on a Diffusion System Spherical Hazemeter were performed to confirm the visual observations.

Morphology

The phase-separated samples were rapidly quenched to a temperature lower than the glass-transition temperature by liquid nitrogen and then sectioned into thin films approximately 90nm thick with a low-temperature LKB 2088 ultramicrotome with a diamond knife. The ultrathin films were attached to copper grid and stained with 1% aqueous OsO4 for 12hours to increase the contrast between two phases. Morphologies were observed with a HITACHI H-860 transmission electron microscope (TEM). The light areas in the resulting micrographs corresponded to the PMMA-rich phase, whereas the dark areas were related to the SMA-rich phase.

Rheology

Rheological measurements were carried out on a rotational rheometer (Bohlin Genemi 200HR) with 25mm parallel-plate geometry. The modes of measurements included:

a) Dynamic strain sweeps at a given temperature and frequency to determine the linear viscoelastic regime;
b) Dynamic time sweeps at a given temperature, frequency and strain in the linear viscoelastic regime to obtain steady state, and thus, to ensure that measurements were performed under dynamic equilibrium conditions;
c) Isothermal dynamic frequency sweeps (0.01-100rad/s) at a given strain in the linear viscoelastic regime at different temperatures from 140 to 230^{o}C by a step of 10^{o}C, to investigate the dynamic mechanical material functions over the whole accessible frequency range.

Results and Discussion

Thermal Analysis and Thermodynamic Phase Diagram

In Figure 1, the glass transition temperatures (T_g) of the PMMA/SMA blends are plotted versus composition. For the samples of all compositions only a single T_g is obtained. Blends exhibiting a single T_g are often regarded as miscible while the immiscible ones are characterized by two distinct values of T_g, corresponding to the two phases. Features of single T_g also corroborate the miscibility of all blends prepared. The composition dependence of the T_g can be good described by the Gordon-Taylor-Kwei empirical equation [27]. In addition, it is noted that the difference in T_g between the blend components. That is generally responsible for the reduced magnitude of the observed rheological response, compared to blends exhibiting much larger contrast in T_g [17].

The stagnant phase diagram shown in Figure 1 was determined through cloud point measurements at a heating rate of 1^{o}C/min. The cloud point was taken as the temperature at which the first sign of cloudiness appears, which corresponds also to the beginning of the decrease in transmitted light. From Figure 1, one can see the

PMMA/SMA blend has a lower critical solution temperature (LSCT) of 204°C, and the critical composition is close to 0.4. The volume fractions were calculated from the weight fractions assuming a vanishing excess mixing volume. The phase behavior of the PMMA/SMA blend was modeled using Flory-Huggins model [28]. The coexistent phases of a binary system are given by the conditions that the chemical potentials of each component are equal in the two phases. By assuming that the Flory-Huggins parameter, χ, depends only on temperature, according to $\chi=A+B/T$ [28], fitting the phase diagram shown in Figure 1 yields the parameters A=0.01407 and B=-4.768K, respectively. The values of A and B obtained are comparable with the results reported by Brannock et al. [29]. In addition, according to phase diagram, once phase separation takes place, the sample always separates into two phases with composition of PMMA-rich ϕ' and SMA-rich ϕ'' at a certain temperature above the binodal curve, regardless of its initial composition. The volume fractions of such two phases can be determined by the lever rule [30].

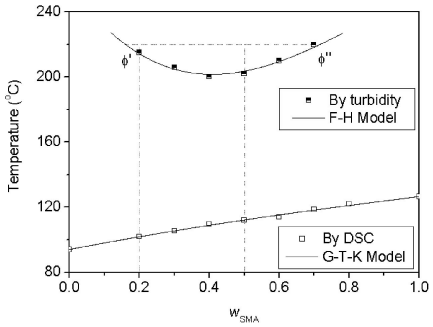

Figure 1 Composition dependence of T_gs and cloud points of the PMMA/SMA blends

Viscoelastic Properties of the Blends in Homogeneous Region

Below 180°C (in homogeneous region), after applications of the time-temperature superposition (tTS) principle [31, 32] based on the William-Landel-Ferry (WLF) equation, the various isotherms were constructed to generate the master curves of the dynamic moduli of the both components and the blends of weight compositions of 80/20, 60/40, 50/50, 40/60, and 20/80, at a reference of 180°C, as shown in Figure 2. Only horizontal shifting along the frequency axis was performed.

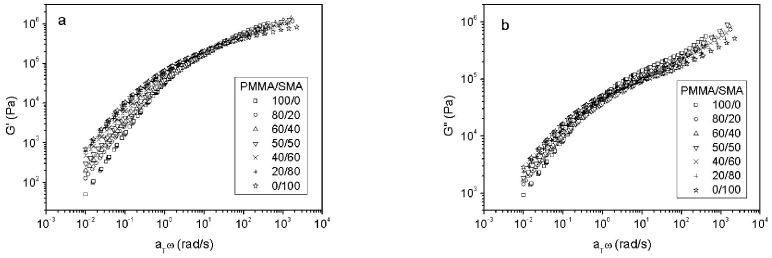

Figure 2 Master curves of G' (a) and G'' (b) of the pure PMMA and SMA and their blends of different compositions at a reference temperature of 180°C

In Figure 2, one can see time-temperature superposition (tTS) principle holds well for all the blends of different composition in homogeneous region. Typical terminal behavior at low frequencies is then observed: $G' \propto \omega^2$ and $G'' \propto \omega$, respectively [31].

Viscoelastic Properties of the Blends in Transitional and Phase-Separated Regions

As temperature increases and approaches the phase separation temperature, the viscoelastic properties of the blend will change dramatically [2-21]. In the following section, we will focus on the blend of 50/50 and 80/20 weight compositions. These two blend series are chosen because they are typical representatives with symmetric and off-symmetric composition.

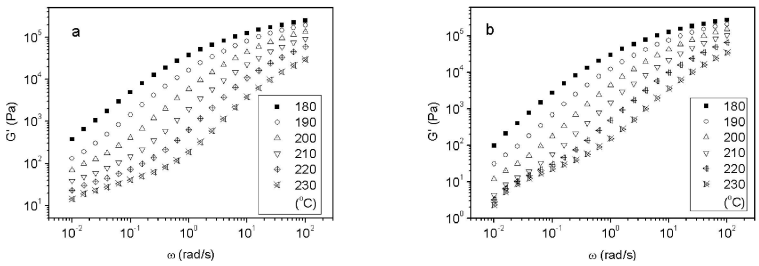

Figure 3 Storage moduli of the 50/50 (a) and 80/20 (b) PMMA/SMA blend at different temperatures

In Figure 3, the storage moduli of the blends of symmetric (50/50) and off-symmetric (80/20) compositions at different temperatures are plotted. One can see, close to and above a certain temperature, the storage modulus of the blend gradually deviates from classical terminal behavior. This behavior is well-documented in the literatures [2-9, 14-17] and represents a fingerprint for the presence of phase-separated domains. The pronounced elasticity is attributed to concentration fluctuation near the phase boundary, and interfacial tension in phase-separated regions [15, 16]. But it is noted that for the blends of symmetric and off-symmetric compositions, their rheological responses in two-phase region are obviously different. The storage modulus, G', of the blend of symmetric composition, displays a power law behavior at low frequencies ($G' \sim \omega^{\beta}$ with $\beta<1$) [7, 8, 13, 21, 23]. On comparing the rheological response with microscopic images of the sample, it was proofed that this feature is the characteristic dynamic response of the co-continuous morphology [8, 13, 23]. Weis et al. [23] attributed this power law behavior to the presence of domains with different characteristic length scales and thus different relaxation times. And in the case of the blend of off-symmetric composition, a shoulder is observed in the low-frequency regimes [1, 3, 8, 15, 16, 21, 23]. This is attributed to shape relaxation of the droplets of the dispersed phase driven by interfacial tension [3, 15, 16], corresponding to the droplet-matrix morphology [23]. Therefore, we think such characteristic rheological behaviors should be the reflections of different morphologies.

In contrast to G', the loss modulus, G'', remains almost unchanged and shows no anomalous terminal response, even deep into the phase-separated region, as illustrated in Figure 4. G'' has been shown either insensitive or very weakly sensitive to phase separation [2-23].

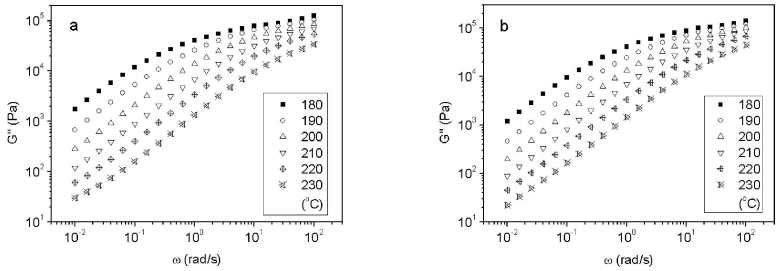

Figure 4 Loss moduli of the 50/50 (a) and 80/20 (b) PMMA/SMA blend at different temperatures

Master Curves

In the case of heterogeneous polymer materials, in particular polymer blends, the different phase domains of the material in general display a different temperature dependent rheology, so that tTS will not hold for blends [32]. That is why the failure of the tTS was often used for characterizing phase separation [2, 3-7, 15-17, 21]. However, if all relaxation mechanisms are similar, the relaxation spectrum at different temperatures does not change in form and in amplitude, and it is only translated on the time scale, tTS will still hold well [32]. That means the validity of tTS does not necessarily warrant that the blend system is a homogeneous one. In practice, several results of the literatures reported the validity of tTS even for multiphase systems [32]. Conversely, the failure of tTS certainly means some structural changes occurred in the blend systems, and phase separation is more likely to be considered as the cause of the failure of tTS in polymer blends [4]. In general, master curves must be constructed through horizontal and vertical shifts in order to test the validity of tTS.

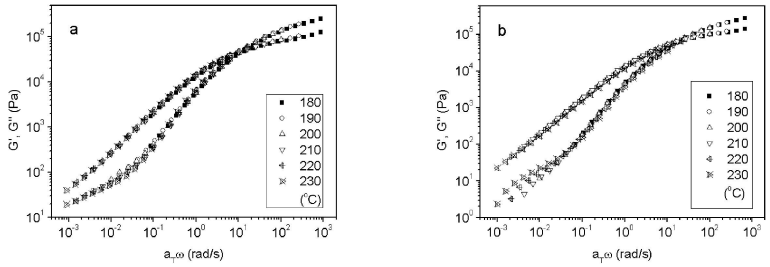

Figure 5 Master curves of G' and G'' of the 50/50 (a) and 80/20 (b) PMMA/SMA blends at a reference temperature of 200°C

Figure 5 shows the master curves of G' and G'' of the samples of symmetric and off-symmetric compositions as a function of the reduced angular frequency at a reference temperature of 200°C, which covers both the homogenous and phase-separated regions. For the sample of symmetric composition, no significant failure of tTS for both G' and G'' in the whole frequency range is observed, even deep into phase-separated regions. Whereas an obvious split of master curves of G' at low reduced frequencies is observed for the sample of off-symmetric composition.

In contrast to these, the failures of tTS principle were always evidently observed for the polystyrene/poly(vinyl methyl ether) blends of both near-symmetric (60/40) and

off-symmetric (80/20 or 20/80) composition [15, 16]. As mention above, even for the blends of different initial compositions, the compositions of the two phases separated into are the same. Then the resulting morphology should be responsible for whether the failure of the tTS is evident or not. This explains why the failures of tTS principle of the blend systems investigated by Chopra et al. [5] and Jeon et al. [7] were not evident, too. On the other hand, since the volume fraction of the two phases separated into is determined by the phase diagram as mention above, considering the off-symmetric phase diagram contrary to the near-symmetry one in the present case, the evident failure of tTS for the blend of near-symmetric (60/40) composition [16] is reasonable.

Han Plots

According to the rheological criterion established by Han et al. [33-39], the plot of $\log G'$ versus $\log G''$ (so-called Han plot) must not only be temperature independent but also have a slope of 2 in the terminal region if a blend is regarded as being truly homogeneous.

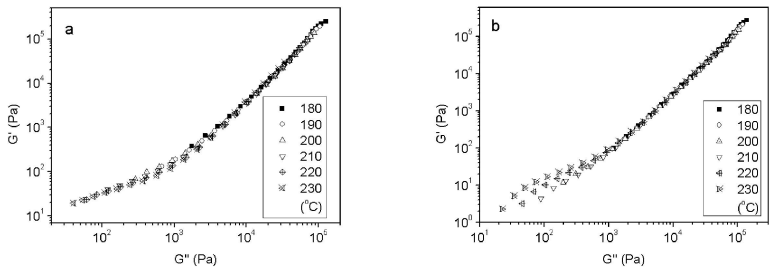

Figure 6 Han Plots for the 50/50 (a) and 80/20 (b) PMMA/SMA blend at different temperatures

Figure 6 depicts this representation for the sample of symmetric and off-symmetric compositions at different temperatures, which covers both the homogenous and phase-separated regions, too. Similar behaviors with the master curves are observed: for the samples of symmetric composition, the experimental data obtained at different temperatures superpose nearly on the same curve, and show a temperature independent behavior; and for the samples of off-symmetric composition, the curves break evidently down. Certainly, the slopes of the curves deviate gradually from 2 with increasing temperature. Han plots were thought to be more sensitive than master curves to be used for judging phase separation [9, 12]. But that is not the case in the present research. But not matter what, the samples of different compositions still display evidently different features.

van Gurp-Palmen Plots

Except for the master curves, van Gurp and Palmen presented a new analysis to check the validity of tTS principle [32]. They plotted the phase angle, δ, as a function of the absolute value of the complex modulus, $|G^*|$ (so-called van Gurp-Palmen Plot) for different temperatures. Various isotherms will superpose nearly on the same curve if tTS principle holds. This way of plotting eliminates the effect of shifting along the frequency axis, and yields temperature independent curves when tTS holds. Therefore, failure of TTS can conveniently be read from them. The plots were also used as a tool

to investigate compatibilization of immiscible blends by Macabucas et al. [40]. However, Friedrich et al. found it is very useful to characterize polydispersity of linear polymers, and to classify topology of long-chain branching [41-43]. We notice that terminal response of phase-separated blend in rheology is similar with long-chain branching, and should show characteristic shape in van Gurp-Palmen plot.

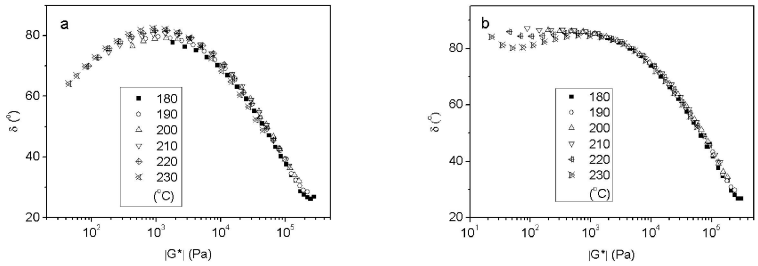

Figure 7 van Gurn-Palmen Plots for the 50/50 (a) and 80/20 (b) PMMA/SMA blend at different temperatures

As illustrated in Figure 7, above a certain temperature, that is, in phase-separated state, the curves don't merge into a single curve, and show a temperature dependent behavior, which means tTS does not hold. It is should be pointed out van Gurm-Palmen Plots seem to be more sensitive than mater curves to test the validity of tTS principle. In general, the curve of the homogeneous linear polymer melt finally reaches a plateau at 90^o when going from high to low |G*|-values in general [42]. In contrast to that, such plots of the two-phase samples exhibit characteristic shapes in low |G*|-regions. The phase-separated samples of symmetric composition, pass a maximum, and then descend with decreasing |G*|, whereas the phase-separated ones of off-symmetric composition have a developed vale between the maximum and the 90^o plateau. These characteristic behaviors should be corresponding to a droplet-matrix or co-continuous morphologies, respectively.

Cole-Cole Plots

It has been well-known that the plot of η'' versus η' (where $\eta'' = G'/\omega$ and $\eta' = G''/\omega$, so-called Cole-Cole plot) can also be used for characterizing the two-phase structure of polymer blends [5, 21]. As shown in Figure 8, below a certain temperature, that is, in homogeneous region, there is only one circular arc in the curve. Above this temperature, a tail or a second circular arc appears on the right-hand side of the arc, corresponding to the sample of symmetric or off-symmetric composition, respectively, which indicates a second relaxation mechanism appears and denotes a second phase forms [5, 21]. Such plots in the phase-separated region clearly display two different relaxation mechanisms corresponding to the two different phase domains [44]. However, it is noted that for the samples of symmetric and off-symmetric compositions, Cole-Cole Plots in phase-separated regions display two different characteristic shapes. For the former, a tail is always observed on the right-hand side of the main arc, even deep into two-phase regions, whereas a second arc, even close to phase boundary. We propose these should be the reflections of the different internal structures. That means that the droplet-matrix and co-continuous morphologies should be responsible for such features.

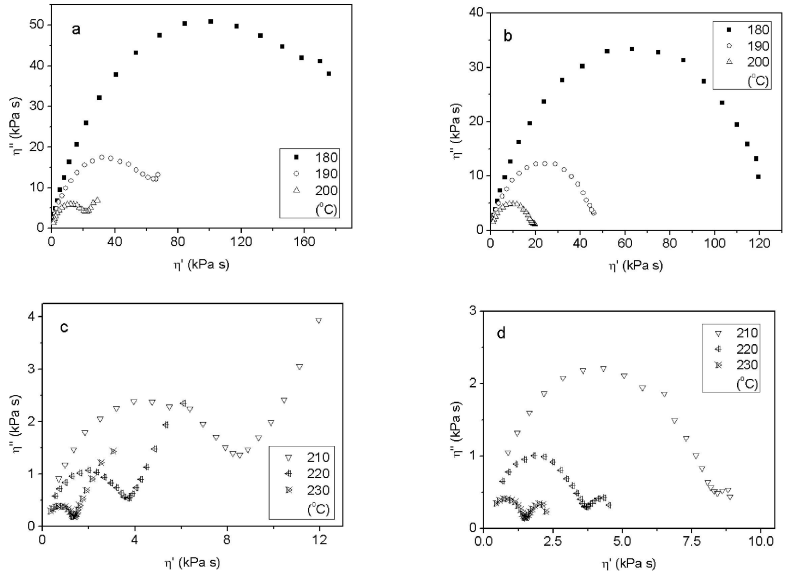

Figure 8 Cole-Cole Plots for the 50/50 (a, c) and 80/20 (b, d) PMMA/SMA blend at different temperatures

Morphology Analysis

In order to confirm our speculation, we have investigated the resulting morphologies of the phase-separated samples at 220°C with TEM. As shown in Figure 9, co-continuous and droplet-matrix domains are observed for the initial 50/50 and 80/20 PMMA/SMA blends, respectively. In part a of Figure 9, it seems that the PMMA-rich phase (light region) dominates at a glance, however, that is not the case. That is because only maleic anhydride (MA) monomer can be stained and the present SMA contains only 12 wt% MA, thus phase contrast between PMMA and SMA is not enough large. After image analysis in detail, we think the SMA-rich phase is really dominant, which is accordance with the estimation based on phase diagram shown in Figure 1. In part b of Figure 9, the SMA-rich region is undoubtedly dispersed phase. These observations confirm that the co-continuous and droplet-matrix morphologies are responsible for the characteristic complex rheological behaviors mentioned above.

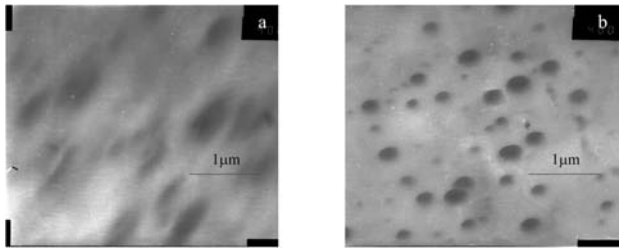

Figure 9 TEM pictures of phase-separated 50/50 (a) and 80/20 (b) PMMA/SMA blend at 220°C (The dark areas denote the SMA-rich domains.)

Model Analysis

As mentioned above, in phase-separated regime, the underlying characteristic is the enhanced storage moduli (at low frequencies), which is attributed to interfacial tension. It is clear that the phase morphology is the key parameter responsible for the thermorheological complexities of the phase-separated blends. Such complex viscoelastic behavior can be quantitatively described by utilizing Palierne's emulsion model [44]. Under the assumptions that the deformation of the inclusions remains small, within the limits of linear viscoelasticity and the dispersed droplets are nearly monodisperse, the linear complex shear modulus of the blend is expressed by [45]

$$G_b^*(\omega) = G_m^*(\omega)\frac{1+3\phi H(\omega)}{1-2\phi H(\omega)} \tag{1}$$

with $$H(\omega) = \frac{4(\alpha/R)[2G_m^*(\omega)+5G_d^*(\omega)]+[G_d^*(\omega)-G_m^*(\omega)][16G_m^*(\omega)+19G_d^*(\omega)]}{40(\alpha/R)[G_m^*(\omega)+G_d^*(\omega)]+[2G_d^*(\omega)+3G_m^*(\omega)][16G_m^*(\omega)+19G_d^*(\omega)]} \tag{2}$$

where $G_b^*(\omega)$, $G_m^*(\omega)$, and $G_d^*(\omega)$ are the complex shear moduli of the blend, the matrix and the dispersed phase, respectively, ϕ denotes the volume fraction of the inclusions of size R, and α is the interfacial tension between the dispersed phase and the matrix. This approach was used for the case of immiscible polymer blend. On the one hand, given results from dynamic measurements and information about the size of the inclusions which can be obtained from microscopy, interfacial tension can be estimated from this model [7, 46-50]. On the other hand, the sphere-size distribution of inclusions can even be determined based on this model in combination with the information about interfacial tension [51]. According to the method established by Friedrich et al. [51], one could theoretically obtain the information about morphology if the moduli of the two phases and the interfacial tension between them are known. Due to the phase diagram involved here, the present partially miscible blend will never actually separate into pure PMMA and pure SMA domains; instead, it consists of PMMA-rich and SMA-rich domains with the composition determined by the tie lines of the phase diagram. The dynamic moduli of the two phases are obtained from dynamic measurements of the miscible mixtures with the composition equal to those of the two phases, respectively, at the same temperature. However, there is no available information about interfacial tension of the present polymer blend so far. Therefore, in this work, we employ essentially above equations to the present phase-separated blend to quantify the ratio (α/R).

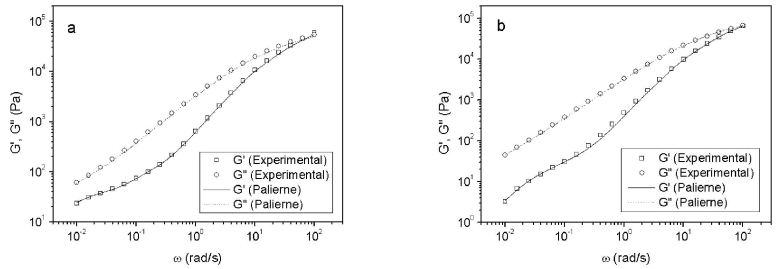

Figure 10 Dynamic moduli of the phase-separated blends containing initial 50/50 (a) and 80/20 (b) PMMA/SMA at 220°C

Application of the above model, with only one adjustable parameter, namely the ratio (α/R), produces the results depicted in Figure 10. With α/R=100 and 200Pa at 220^{o}C, respectively, the best fittings are obtained. Since there is no available information about interfacial tension, no available sphere-size distribution of inclusions can be directly compared with the results from microscopy. However, as mentioned above, the final compositions of the two resulting phases from the samples of different initial compositions are equal respectively at the same phase separation temperature. It is reasonable to assume that the interfacial tensions between two resulting phases from the samples of different initial compositions are equal. Then we conclude that the phase size for the case of symmetric composition is larger than that for the case of off-symmetric composition. This is in qualitative agreement with the observations from microscopy. It should be pointed out that it is not appropriate to employ Palierne's model to the sample with a co-continuous structure, although this model was frequently used without consideration on morphology [7, 16, 46].

Conclusions

In this study, we have presented a detailed rheological investigation of a PMMA/SMA blend showing a LCST behavior. In homogeneous region, the blends of different composition behave as a classical polymer melt. On the other hand, in phase-separated region, Deviations from the classical scaling laws for the storage modulus at low frequencies are observed. The blends of symmetric and off-symmetric composition show different characteristic thermorheological responses. For the former, a power law behavior at low frequencies in the storage modulus curve, the validity of tTS, the temperature independence of Han Plots, a monotonous decreasing at low $|G^*|$-value regions in van Gurn-Palmen Plots, and a tail in Cole-Cole Plots are observed. On the other hand, for the latter, a shoulder in the storage modulus curve, the failure of tTS, the temperature dependence of Han Plots, a developed vale in van Gurn-Palmen Plots, and a second arc in Cole-Cole Plots are observed. TEM analysis confirms that the morphologies of the phase-separated samples are responsible for such fingerprints of these rheological functions, which can be qualitatively corroborated by utilizing Palierne's emulsion model. The comparison of the different correlations between rheological functions has shown that van Gurn-Palmen Plots and Cole-Cole Plots are most sensitive to phase separation and morphology. They are the most appropriate for characterizing phase separation and morphology.

Our work has made clear that rheology is a sensitive tool for an analysis of the structure of materials. Moreover, the success in the qualitative analysis of morphology by rheology made it possible to quantitative rheological evaluation of phase transition in two-phase polymer blends.

Acknowledgements. This research was supported by the National Natural Science Foundation of China (Grant No. 20204007, No. 20474039, and No. 20490220). The polymer SMA samples used were generously donated by SINOPEC Shanghai Research Institute of Petrochemical Technology.

References

1. Bates FS (1991) Science 251: 898
2. Sharma J, Clarke N (20040 J Phys Chem B 108: 13220

3. Du M, Gong J, Zheng Q (2004) Polym 45: 6725
4. Bousmina M, Lavoie A, and Ried B (2002) Macromol 35: 6274
5. Chopra D, Kontopoulou M, Vlassopoulos D, et al. (2002) Rheol Acta 41: 10
6. Du M, Wang L, Yang B, Song X, Zheng Q (2002) Chem J Chin Univ 23: 961
7. Jeon HS, Nakatani AI, Han CC (2000) Macromol 33: 9732
8. Vinckier I, Laun HM (2000) Macromol Symp 149: 151; (1999) Rheol Acta 38: 274
9. Kim JK, Son HW (1999) Polym 40: 6789
10. Kim JK, Son HW, Lee Y, Kim J (1999) J Polym Sci: Part B: Polym Phys 37: 889
11. Chopra D, Vlassopoulos D (1998) J Rheol 42: 1227
12. Kim JK, Lee HH, Son HW (1998) Macromol 31: 8566
13. Polios IS, Soliman M, Lee C, Gido SP, et al. (1997) Macromol 30: 4470
14. Vlassopoulos D, Koumoutsakos A, Anastasiadis SH (1997) J Rheol 41: 739
15. Kapnistos M, Hinrichs A, Vlassopoulos D, et al. (1996) Macromol 29: 7155
16. Kapnistos M, Vlassopoulos D, Anastasiadis SH (1996) Europhys Lett 34: 513
17. Vlassopoulos D (1996) Rheol Acta, 35: 556
18. Nesarikar AR (1995) Macromol 28: 7202
19. Takahashi Y, Suzuki H, Nakagawa Y, Noda I (1994) Polym Inter 34: 327
20. Mani S, Malone MF, Winter HH (1992) J Rheol 36: 1625
21. Ajji A, Choplin L, Prudhomme RE (1991) J Polym Sci: Part B: Polym Phys 29: 1573; (1988) ibid. 26: 2779
22. Fahrlander M, Friedrich C (1999) Rheol Acta 38: 206
23. Weis C, Leukel J, Borkenstein K, Maier D, et al. (1998) Polym Bull 40: 235
24. Steinmann S, Gronski W, Friedrich C (2002) Rheol Acta 41: 77
25. Ziegler V, Wolf BA (1999) J Rheol 43: 1033
26. Utracki LA (1991) J Rheol 35: 1615
27. Utracki LA (1990) Polymer Alloys and Blends, Hanser, New York
28. Frory PJ (2003) Principles of polymer chemistry, World Pub. Corp., Beijing
29. Brannock GR, Barlow JW, et al. (1991) J Polym Sci: Part B: Polym Phys 29: 413
30. Paul DR, Newman S (1978) Polymer Blends, Academic Press, New York
31. Ferry JD (1980) Viscoelastic Properties of Polymers (3rd), Wiley, New York
32. van Gurp (1998) Rheol Bull 67: 5
33. Mather PT, Romo-Uribe A, Han CD, Kim SS (1997) Macromol 30: 7977
34. Han CD, Kim SS (1995) Macromol 28: 2089
35. Han CD, Baek DM, Kim JK, Ogawa T, et al. (1995) Macromol 28: 5043
36. Kim SS, Han CD (1993) Macromol 26: 6633
37. Han CD, Baek DM, Kim JK (1990) Macromol 23: 561
38. Han CD, Kim J, Kim JK (1989) Macromol 22: 383
39. Han CD., Kim JK (1989) Macromol 22: 4292
40. Macaubas PHP, Demarquette NR (2002) Polym Eng Sci 42: 1509
41. Schulze D, Roths T, Friedrich C (2005) Rheol Acta 44: 485
42. Trinkle S, Walter P, Friedrich C (2002) Rheol Acta 41: 103
43. Trinkle S, Friedrich C (2001) Rheol Acta 40: 322
44. Palierne JF (1990) Rheol Acta 29:320
45. Graebling D, Muller R, Palierne JF (1993) Macromol 26: 320
46. Khonakdar HA, Jafari SH, Yavari A, et al. (2005) Polym Bull 54:75
47. Lee HS, Kim ES (2005) Macromol 38:1196
48. Vinckier I, Schweizer T, et al. (2002) J Polym Sci Part B: Polym Phys 40:679
49. Lee HS, Denn MM (2000) Polym Eng Sci 40:1132
50. Xing P, Bousmina M, Rodrigue D, Kamal MR (2000) Macromol 33:8020
51. Friedrich C, Gleinser W, Korat E, Maier D, Weese J (1995) J Rheol 39:1411